SVD-Based On-Line Exercise ECG Signal Orthogonalization

Burak Acar and Hayrettin Köymen,* *Senior Member, IEEE*

***Abstract*—An orthogonalization method to eliminate unwanted signal components in standard 12-lead exercise electrocardiograms (ECG's) is presented in this work. A singular-value-decomposition-based algorithm is proposed to decompose the signal into two time-orthogonal subspaces; one containing the ECG and the other containing artifacts like baseline wander and electromyogram. The method makes use of redundancy in 12-lead ECG. The same method is also tested for reconstruction of a completely lost channel. The online implementation of the method is given. It is observed that the first two decomposed channels with highest energy are sufficient to reconstruct the ST-segment and J-point. The dimension of the signal space, on the other hand, does not exceed three. Data from 23 patients, with duration ranging from 9 to 21 min, are used.**

***Index Terms*— Electromyogram (EMG) and baseline wander (BW) elimination, exercise electrocardiogram (ECG), online orthogonalization, signal enhancement, singular value decomposition (SVD).**

I. Introduction

EXERCISE electrocardiogram (ECG) testing reveals very important clinical diagnostic information on cardiovascular disorders. The test itself, however, sets up rather adverse conditions for ECG signal recording. Baseline wander (BW) and electromyogram (EMG) signal contaminates exercise ECG signals. Often the level of contamination is such that ECG signals are completely hidden by these unwanted signal components. Sophisticated signal processing techniques must be employed in order to recover the clinical data.

The most important clinical information is contained in the variation of ST-segment level during the stress test. The ST-segment level is found in all phases of the test, namely the initial resting phase and every step of the exercise and the recovery phases. ST-segment level depression is sought for positive classification. Computerized systems calculate the average beats in successive time intervals, of length ranging from 6 to 20 s. This averaging is necessary since there exist large amounts of unwanted signal components in recordings taken during exercise. ST-level measurements are made on these average complexes.

Various aspects of ECG signal enhancement had been discussed in literature [1]–[11]. Mertens *et al.* used a hybrid approach, which is a combination of mean and median filtering [12]. Pinto proposed a BW filter and a time-varying filter to remove high-frequency EMG signal [13]. Sornmo estimated the BW from a QRS-free signal obtained by subtracting the average beat from the incoming noisy beat and used this to remove the BW [14]. Mortara proposed an approach to obtain a transfer function of the cardiac dipole, which he referred to as source consistency filtering [15]. Jane *et al.* used a cascade of two adaptive filters to remove BW and gave a comparison of this to cubic spline filter [16] whereas Meyer *et al.* used a cubic spline technique to estimate and remove BW from ECG [17]. Recently, Afonso *et al.* proposed a filter-bank-based approach for the processing of stress ECG [18]. They decomposed the signal into different subbands and processed each subband independently.

The proposed methods provided enhancement of ECG data at varying levels. The efforts for enhancement were confined to processing of individual derivations, in all of these methods. There is, however, a significant redundancy in 12-lead ECG, which can contribute to unwanted signal interference elimination when all derivations are processed simultaneously. Barr *et al.* addressed this redundancy while they investigated the optimum lead locations for complete representation of total body QRS surface potential distribution [19]. As far as standard leads are concerned, Barr *et al.* observed that this representation is rather poor. Lux *et al.* made use of the redundancy in a data set of 221 patients. This data consists of a set of approximately 600 body-surface potential maps recorded from 192 leads on every patient [20]. All of these maps are derived from measurements of potentials at every millisecond and within a single heartbeat. In their study, the spatial redundancy in body-surface potential maps is employed to obtain a set of orthonormal basis vectors to represent all the data on all the patients, using Karhunen–Loeve technique. Evans *et al.* employed the same technique on the same population to investigate the temporal redundancy in body surface recordings [21]. It is shown in [21] that the two sets of orthonormal basis vectors are necessary, one for QRS region and one for ST and T regions, to represent all the data accurately over the patient population. It must, of course, be noted that in [21], again, the analyzed data is confined to a period of a single heartbeat.

In this paper, we propose a robust method particularly to obtain ST-segment level data during exercise test. The method makes use of the redundancy in standard leads to eliminate BW, EMG, and other interference in stress ECG. Presence of these unwanted signal components, originating

Manuscript received May 21, 1997; revised September 17, 1998. *Asterisk indicates corresponding author*.

B. Acar is with the Electrical and Electronics Engineering Department, Bilkent University, Ankara 06533, Turkey.

*H. Köymen is with the Electrical and Electronics Engineering Department, Bilkent University, Ankara 06533, Turkey (e-mail: koymen@ee.bilkent.edu.tr).

Publisher Item Identifier S 0018-9294(99)01847-9.

from independent sources, in stress ECG, establish different problems compared to rest ECG signals. The method employs time domain orthogonalization technique in order to reduce the ECG data to a set of two or three time-orthogonal signals, for every patient and for the entire duration of stress test. We employed a recursive orthogonalization algorithm that approximates singular value decomposition (SVD); first proposed by Vanderschoot *et al.* [22] to separate fetal and maternal ECG signals. We observed that ECG waveforms in 12 standard leads decompose into at most three orthogonal signals per patient. The morphology of these three signals, however, varies from patient to patient.

The morphology of ECG waveform and, hence, the values of clinical parameters change during exercise testing. The method we proposed can accommodate this property of ECG waveform during exercise testing.

Another difficulty in exercise testing is that one or more channels can be lost temporarily or completely during the test. The said redundancy can be used to recover the clinically important part of the data. We tested the same orthogonalization method for this purpose.

We implemented the method in C programming language. It is possible to process standard 12-lead ECG data in real-time on any personal computer with a Pentium microprocessor. SVD orthogonalization algorithm used in this work is given in Ssection II. The details of the way we used this technique are explained in Section III. We discuss the results that we obtained from 23 patients in Section IV.

II. Theory: Time Domain Orthogonalization of Long ECG Records

The cardiac signal morphologies in standard 12-lead ECG signals are highly correlated. Eight channels out of 12 are independent and orthogonalization is applied to these eight channels. These are DI, DII, and V1–V6.

We consider the entire data recorded during exercise test as a data matrix **M.** Each row of **M** corresponds to an input channel, whereas columns correspond to successive sampling instants in time. The algorithm is based on the online approximation of SVD of the data matrix $\mathbf{M} \in \mathbf{R}^{p\times n}$.

SVD of **M**, in general, is given in [23] as

$$\mathbf{M} = \mathbf{U}\boldsymbol{\Sigma}\mathbf{V}^T \tag{1}$$

$$\mathbf{U}\mathbf{U}^T = \mathbf{U}^T\mathbf{U} = I_p, \qquad \mathbf{V}\mathbf{V}^T = \mathbf{V}^T\mathbf{V} = I_n \tag{2}$$

where the columns of **U** and **V** are the left and right singular vectors, respectively. $\boldsymbol{\Sigma}$ is a diagonal matrix whose diagonal entries are the singular values of **M**. If the rank of **M** is r, then

$$\widetilde{\mathbf{U}}_r = \text{span}(\mathbf{u}_1, \cdots, \mathbf{u}_r) \tag{3}$$

spans the range of **M** and $\widetilde{\mathbf{U}}_r\widetilde{\mathbf{U}}_r^T$ projects **M** onto that subspace. The relation between the eigenvalue decomposition and SVD can be established from (1) as

$$\boldsymbol{\Sigma}^2 = \mathbf{U}^T\mathbf{M}\mathbf{M}^T\mathbf{U}. \tag{4}$$

The complete **M** matrix is available only at the end of the test. During the test, each column of **M** is received one after the other. The proposed algorithm approximates (1) at every sampling instant.

The algorithm is given by

$$\mathbf{U}_0 = \mathbf{I}, \qquad \mathbf{C}_0 = \mathbf{0} \tag{5}$$

$$\text{for } i = 1 \text{ to } n \tag{6}$$

$$\mathbf{s}_i = \mathbf{U}_{i-1}^T\mathbf{m}_i \tag{7}$$

$$\mathbf{B}_i = \alpha^2\mathbf{C}_{i-1} + \mathbf{s}_i\mathbf{s}_i^T \tag{8}$$

$$\mathbf{C}_i = \mathbf{Q}_i^T\mathbf{B}_i\mathbf{Q}_i \tag{9}$$

$$\mathbf{U}_i = \mathbf{U}_{i-1}\mathbf{Q}_i \tag{10}$$

$$\hat{\mathbf{m}}_i = \mathbf{U}_{i-1}\hat{\mathbf{s}}_i \tag{11}$$

where

$$\mathbf{m}_i = i\text{th column of } \mathbf{M} \tag{12}$$

$$r = \text{rank}(\mathbf{M}) \tag{13}$$

$$\hat{\mathbf{s}} = [s_1 \cdots s_r\, 0 \cdots 0] \tag{14}$$

$$\mathbf{U} = \left[\widetilde{\mathbf{U}}_r\, \widetilde{\mathbf{U}}_n\right] \tag{15}$$

$$\mathbf{Q}_i = \text{Jacobi rotation matrix.} \tag{16}$$

The matrix **U** corresponds to the left singular matrix. The matrix **C** is an approximation to $\boldsymbol{\Sigma}^2$, whereas the matrix **B** is an intermediate matrix and is an updated version of **C** in each step. The matrix **C** converges to the matrix $\boldsymbol{\Sigma}^2$ in (4). The convergence rate is determined by α, the forgetting factor. The choice of α is important since it determines the amount of history that the algorithm takes into account. This choice describes the preference between stability of the algorithm and its adaptability to the variations in the morphology of the beat. $\mathbf{Q}_i$ is the Jacobi rotation matrix that nullifies an off-diagonal element of $\mathbf{B}_i$ [24]. The off-diagonal element of $\mathbf{B}_i$, whose absolute value is maximum, is chosen to be made zero at each step in the above algorithm. Thus, at each step we decrease the correlation between the most correlated two output channels. In effect the algorithm performs (18) incrementally.

Let

$$\widehat{\mathbf{M}}_i = \left[\alpha^{i-1}\mathbf{m}(t_1), \alpha^{i-2}\mathbf{m}(t_2), \cdots, \mathbf{m}(t_i)\right] \tag{17}$$

$$\mathbf{C}_i = \mathbf{Q}_i^T \cdots \mathbf{Q}_1^T\widehat{\mathbf{M}}_i\widehat{\mathbf{M}}_i^T\mathbf{Q}_1 \cdots \mathbf{Q}_i \tag{18}$$

$$\widehat{\mathbf{U}}_i = \mathbf{Q}_1 \cdots \mathbf{Q}_i \tag{19}$$

$\widehat{\mathbf{U}}_i$ is closer to $\mathbf{U}_i$ than $\widehat{\mathbf{U}}_{i-1}$ where $\mathbf{U}_i$ is defined as

$$\mathbf{U}_i^T\mathbf{M}_i\mathbf{M}_i^T\mathbf{U}_i = \boldsymbol{\Sigma}^2 \tag{20}$$

with

$$\mathbf{M}_i = [\mathbf{m}(t_1) \cdots \mathbf{m}(t_i)]. \tag{21}$$

The correspondence between this approximation and regular SVD is extensively discussed in [22] and is shown to be a very good approximation.

The reconstruction step is given by (11). $\widetilde{\mathbf{U}}_r$ corresponds to high singular values and spans the signal space. $\widetilde{\mathbf{U}}_n$ is its orthogonal complement and spans the noise space. We will refer to the corresponding channels as noise channels. The dimension of the signal space is given by the rank of **M.** The effective rank of **M** is determined by observing the singular values of **M** [23], [25]. In $\hat{\mathbf{s}}$, zeros are substituted for noise channels.

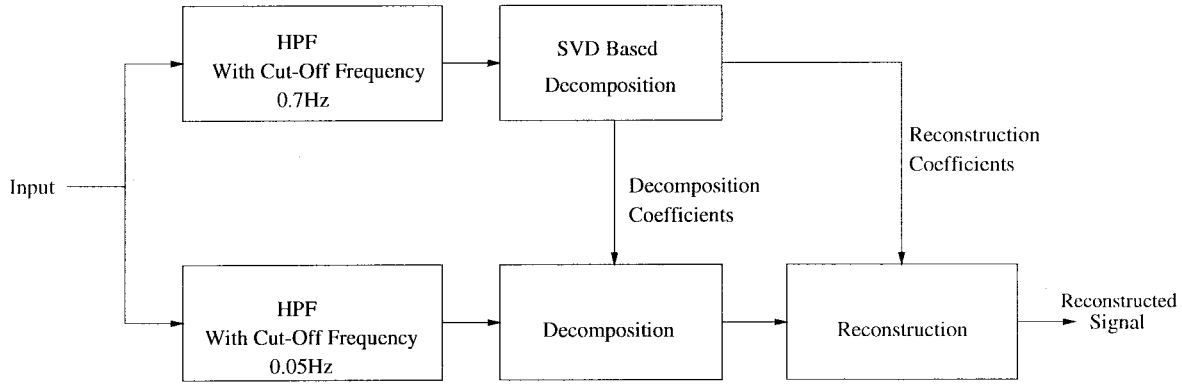

Fig. 1. Block diagram.

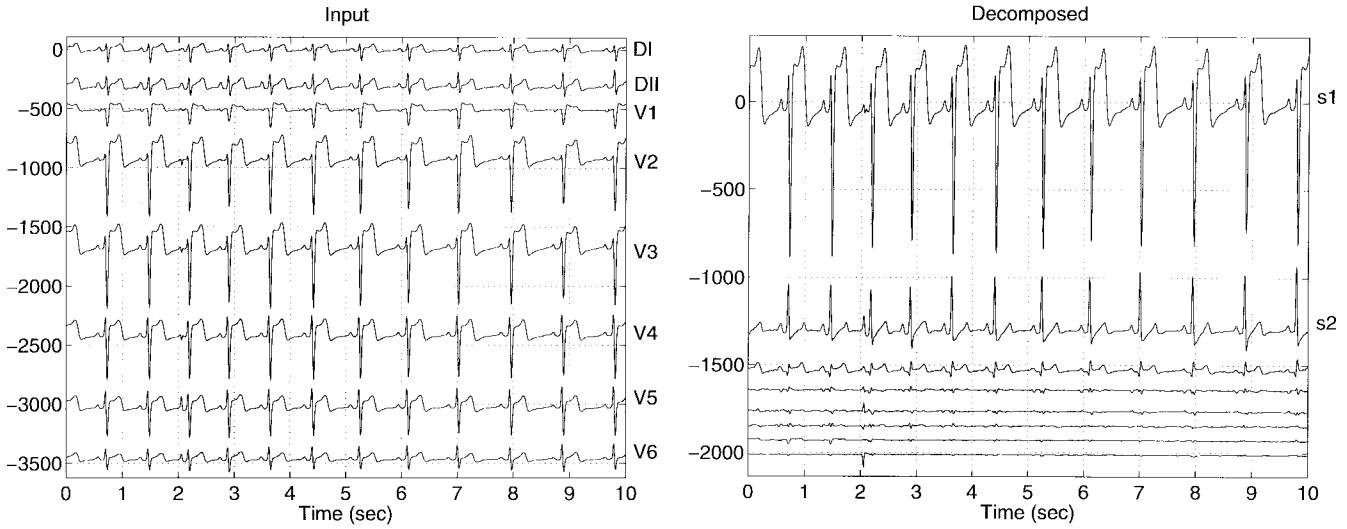

Fig. 2. Eight channel rest ECG.

III. The Method

We processed exercise ECG data records from 23 patients with record lengths between 9:00 and 21:00 min. The data are recorded with a sampling rate of 500 samples/s per channel, at 12 bits resolution under Bruce protocol. The data of eight independent channels in standard 12-lead ECG are acquired simultaneously.

SVD is sensitive to the average value of the input signals. When the derivations contain a nonzero average or very low-frequency components, SVD algorithm decomposes these as orthogonal components. Such low-frequency components increase the rank of the data matrix and dimension of the signal space. This complicates the separation of signal and noise spaces. The input signals are, therefore, first high-pass filtered with a filter of cutoff frequency 0.7 Hz, to remove these low-frequency components. The decomposition coefficients obtained on this signal are applied to the input signals that are high-pass filtered with a first-order filter of cutoff frequency 0.05 Hz. 0.05 Hz is the allowed cutoff frequency in order to preserve all of the clinical data in ECG. The block diagram of the process is given in Fig. 1.

We tested the decomposition capability of the algorithm on rest ECG recordings taken from 23 patients. These signals were free from any visible interference or noise. These experiments showed that at least 99% of the total energy is confined to the first three channels. Fig. 2 shows the original input and the decomposed signal sets. It can be observed that almost all of the energy is contained in the first three decomposed signal channels, while some residue of QRS complexes can be observed on the other five channels. In this paper, the first three decomposed signals are referred to as the signal channels and the space spanned by them as the signal space. We will refer to all unwanted signals such as BW, EMG, and other types of interference as unwanted noise components throughout this paper.

The algorithm requires a training period. The signal morphology and the dimension of the signal space are determined by the algorithm at the end of this period. These decisions are made by observing the levels of singular values. In an ECG signal with almost no unwanted signal components, such as the one taken from a patient under resting conditions, one gets either two or three large singular values that correspond to the signal space. One also obtains five small singular values, largest of which is less than 25% of the smallest signal singular value and less than 1% of the largest signal singular value. When the original ECG signal is contaminated with unwanted

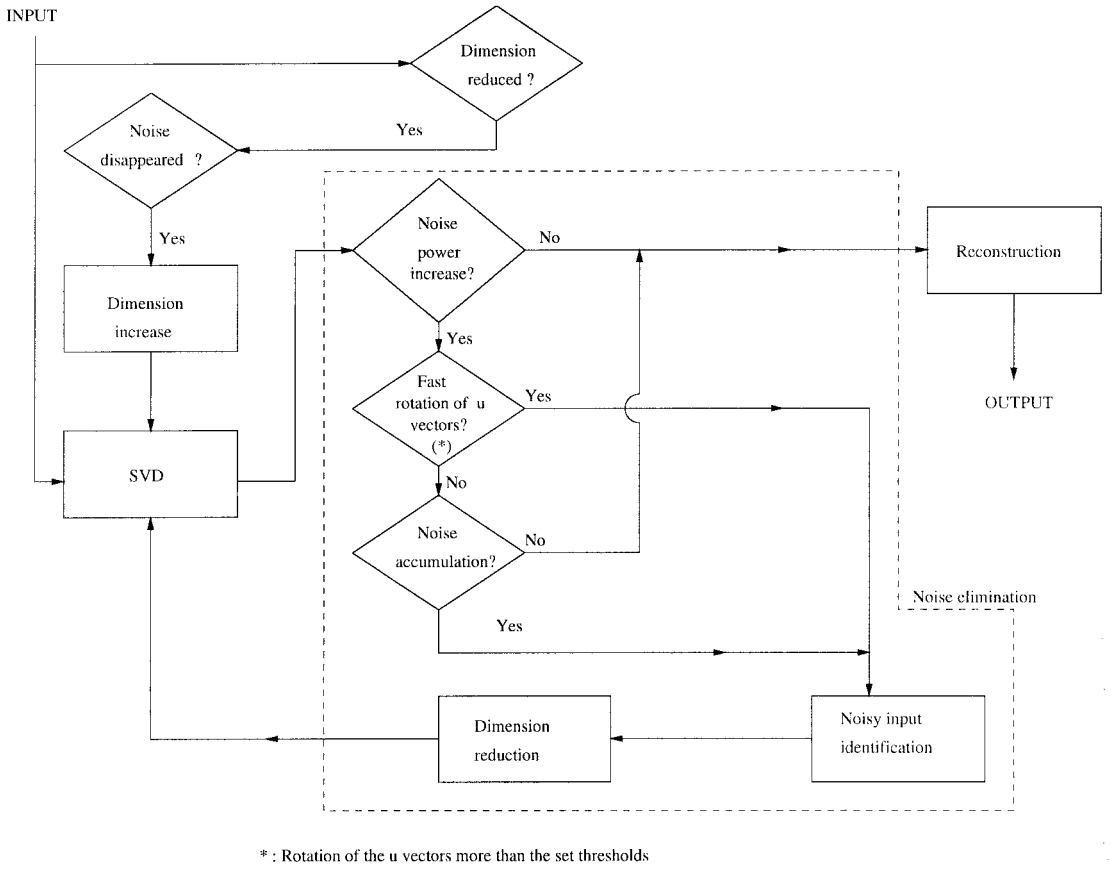

Fig. 3. Flow diagram of the implementation.

signal components, the singular values of the signal space remain the same while the ones corresponding to the noise space increases.

This is due to the fact that unwanted signal components that are time-orthogonal to ECG signals are mapped into the noise space. Whenever the singular values of the noise space exceed those of the signal space, unwanted signal components begin to interfere with the signal components. Such a case can be due to the presence of unwanted components either with a low amplitude and a long persistence or with a high amplitude. We avoided such interference to occur in the algorithm by using rules and thresholds that are determined empirically.

The orthogonalization algorithm is implemented such that it automatically adapts itself to variations in ECG and unwanted signal components. Various limits and thresholds are imposed on the operation of the algorithm in order to maintain the stability against various effects that are encountered during exercise testing. Each of these effects is discussed in the paper. The flow diagram of the implementation is given in Fig. 3.

A. Morphological Variation in ECG Signal During Exercise

The changing shape of the ECG waveform, particularly changes that take place in ST-segment, provides the most important clinical information in exercise testing. These changes obviously affect the orthogonal-basis vectors $\mathbf{u}_i$'s. We observed the changes that take place in $\mathbf{u}_1$, $\mathbf{u}_2$, and $\mathbf{u}_3$ on complete test data which was reasonably free of BW and

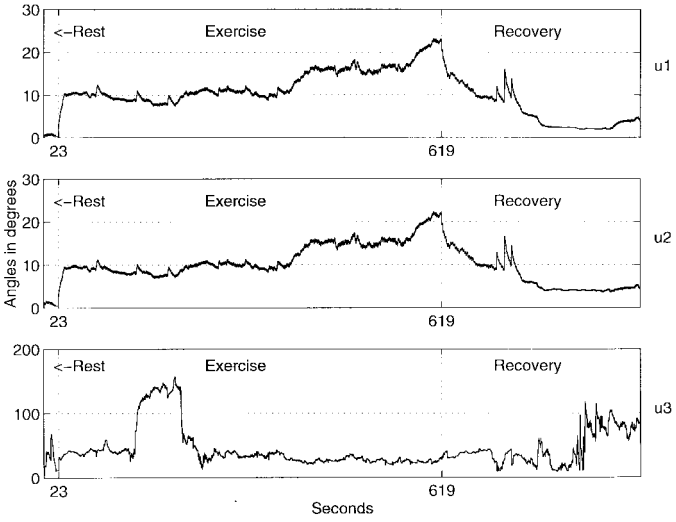

Fig. 4. Directions of first three basis vectors.

EMG signal. In Fig. 4, an example of the variation in the direction of $\mathbf{u}_1$, $\mathbf{u}_2$, and $\mathbf{u}_3$ are given with respect to time. We calculated the angle between the current vector and the vector just before the end of the rest phase, for each time instant and for each one of the three basis vectors, $\mathbf{u}_1$, $\mathbf{u}_2$, and $\mathbf{u}_3$. It can be observed that although there is not any observable change during rest, the orientation of all three vectors change as soon as the exercise phase begins. The directions of $\mathbf{u}_1$ and

$\mathbf{u}_2$ assume new values during each exercise step and stabilize fairly quickly at that value. When recovery phase starts, $\mathbf{u}_1$'s and $\mathbf{u}_2$'s directions gradually change back to their rest values. The changes in $\mathbf{u}_3$ are mainly dominated by the amount of unwanted signal components mapped onto the third signal channel.

B. Elimination of Unwanted Signal Components

The algorithm is capable of mapping the unwanted components and the ECG onto orthogonal subspaces separately. In some cases, shifts between the two subspaces can occur and interference can be observed in the signal space. This is caused by the emergence of unwanted signal components, such as BW and EMG, in the majority of the input channels or in one input channel but with high amplitude. As far as the algorithm is concerned, the amount of emerging unwanted components must be sufficient to rotate the **u** vectors significantly in order to be effective. Tracking these rotations is a reliable method for their detection.

In a rest ECG, the direction of the basis vectors of the signal space, $\mathbf{u}_i^r$ ($i \leq \text{rank}(\mathbf{M})$), fluctuate within 1°. This direction is monitored in 23 patient data, including the records with arrhythmic morphology changes, and this limit is observed experimentally. All changes in ECG morphology of cardiac origin and rhythm are maintained in these three decomposed time-orthogonal basis signals.

Whenever a high-amplitude interfering component emerges, components of **U** rotate quickly. The direction of rotation is such that $\mathbf{u}_i^r$ begin to map these components onto the signal space. Simultaneously, ECG signals are mapped onto the noise space to preserve orthogonality. The level of the rotation indicates the presence of unwanted signal components that will be mapped onto the signal space, while the direction of this rotation reveals the input channel where these unwanted components emerged.

A similar fast rotation of $\mathbf{u}_i^r$ is observed when a channel is lost completely. A channel's data is lost during the exercise if a lead gets loose. SVD considers this lack of ECG waveform as an independent signal and modifies **u** vectors radically. Hence we used a limit on the speed of rotation, in order to detect the presence of effective interference or a lost input channel. This limit is determined as 2°/s, experimentally.

The singular value of each channel is a measure of the energy of the signal in that channel. When a low-amplitude interfering component emerges, it is directly mapped onto the noise space. Those entries of **C** matrix which correspond to the noise channels increase. If such an interference lasts for a long time, energy of that unwanted signal component accumulates and the singular value of this channel increases. When it becomes comparable to that of the signal channel with the lowest energy, these unwanted signal components will eventually be mapped onto this signal channel. We refer to this case as accumulating noise. The rotation speed of the basis vector is low. The accumulation of this type of interference can be detected by observing the growth in the energy of the third signal channel. The decision rule is as follows: The diagonal entry corresponding to the largest noise channel (c_{nn}) is compared to 3% of the sum of the two diagonal entries of **C** corresponding to the two largest signal channels ($c_{11}+c_{22}$).

When the accumulation threshold is violated, the highest component of $\mathbf{u}_i^n$, of that particular decomposed channel, indicates the input channel where the contamination is.

Once the source is determined, the dimension of the decomposition ($\mathbf{M}$) is reduced by one and the channel that contains the noisy signal is excluded from the input signal set. This excluded channel is treated as a completely lost channel from then on, and is reconstructed using the information contained in other channels only. Since the reconstruction coefficients are observed to be almost constant within one exercise step, when there is no unwanted signal interference, we keep the most recent reconstruction coefficients of the lost channel constant during this period. The contaminated input channel is continuously checked for the persistence of contamination. The algorithm monitors the presence of unwanted signal components by calculating the cross-correlation of successive QRS complexes in the contaminated input channel. This calculation is performed once in every 10 s. The detection and alignment of the complexes for correlation are done on the first decomposed signal channel, which is always free of unwanted signal components and has the highest amplitude. When the contamination in that input channel disappears, it is included into the calculations by increasing the dimension. Whenever we need to increase the dimension, algorithm uses the most recent full dimension matrices before dimension reduction. The accuracy of the reconstructed lost channel can only be maintained if the loss period is confined within an exercise step.

We used another limit to maintain the order in signal space. The diagonal elements c_{11} and c_{22} represent the energy contained in two primary decomposed signal channels. If c_{11} and c_{22} are close to each other, the first and second decomposed channels contain comparable amounts of ECG signal energy. When an interfering unwanted signal component exists in the second decomposed signal channel, this may cause c_{22} to exceed c_{11} and, hence, change the order of the first two signal channels. Since these vectors span the signal space, such a rotation does not affect the energy content of the signal space. However this type of rotation may cause false noise alarms. We avoided such false alarms by limiting the rotation angle in **Q**, whenever c_{12} is to be nullified. These two channels are allowed to rotate simultaneously at most at a rate of 0.5°/s. This limit is the maximum rotation speed observed on the records with well-separated signal singular values, where such order exchange does not occur.

Both of these limits, 2°/s and 0.5°/s, are imposed on the speed of rotation of $\mathbf{u}_1$ and $\mathbf{u}_2$. These limits are larger than the speed of rotation that takes place at the beginning of each exercise step explained in Section III-A.

Fig. 5 is a typical example of the accumulation effect of BW. In this data set, there is high amplitude, low-frequency BW in DI, and low-amplitude BW in DII. The ECG energy in the third signal channel is relatively small, and it is not immune to the interference BW as well as other signal channels. If the rotation of $\mathbf{u}_3$ is limited to 0.5°/s, such an interference can be avoided. This situation is depicted in Fig. 5. As a result BW

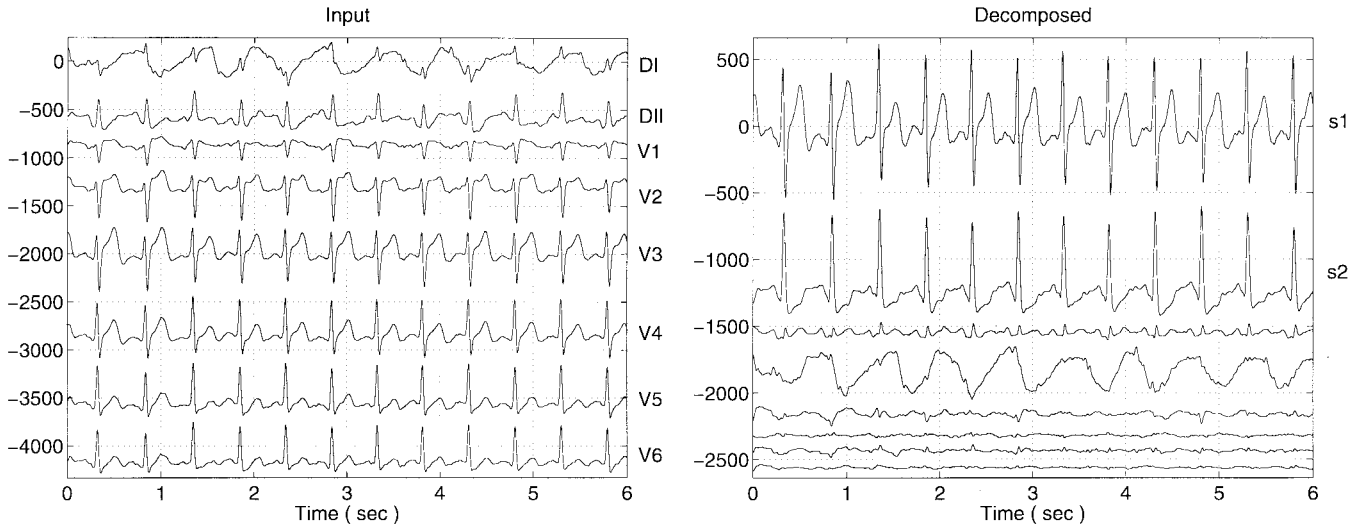

Fig. 5. BW-contaminated ECG.

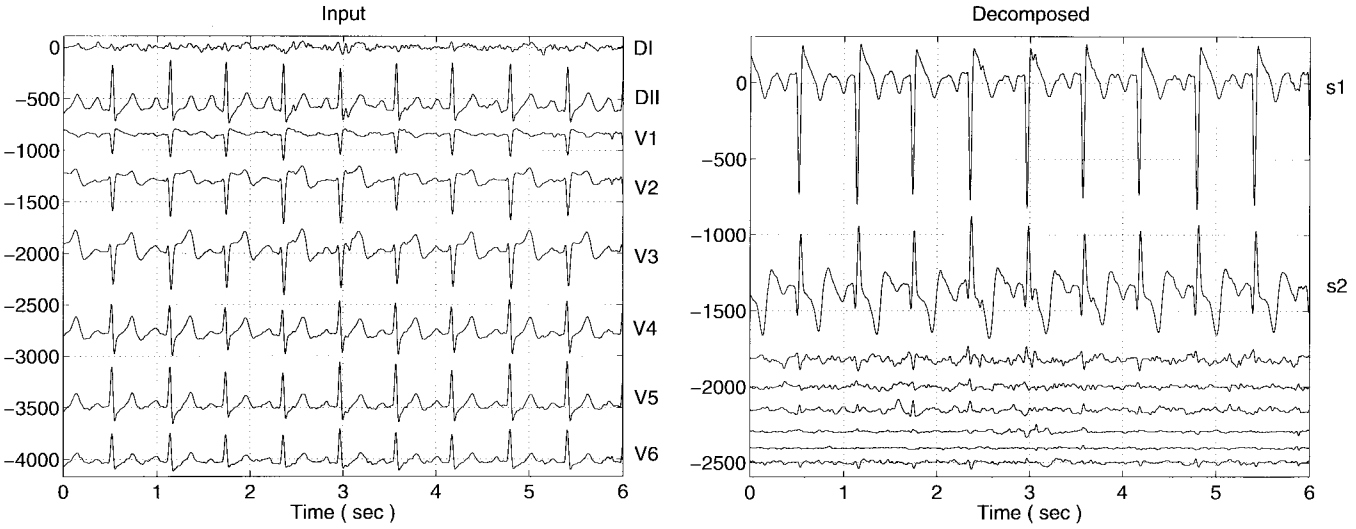

Fig. 6. EMG-contaminated ECG.

is kept mainly in the first noise channel. The residual ECG in that channel is insignificant even when compared to the low energy ECG signal preserved in the third signal channel. In the absence of this limit, the BW observed would appear on the third signal channel.

In Fig. 6, a typical example of the EMG signal mapped onto the noise space is depicted. The low-amplitude EMG is present mainly in DI and partly in DII. With a proper choice of α, this type of interference does not rotate **u** vectors and does not cause an accumulation during the exercise test duration. Rather, it is mapped onto the noise space, to the output channels 4–8. Some contamination in third output channel is observed, while ECG signals free of EMG are maintained in the first two channels.

C. Reconstruction

The original ECG signal and the reconstructed signal are compared in Table I. For this example, the interference content in the original signal is very low in all derivations. The first column contains the mean square difference between the original signal and the reconstructed signal from the two most significant SVD decomposed channels. In certain channels, although one can observe differences up to 3.64%, the morphology of the reconstructed signal does not deviate from the original during QRS complex and ST-segment. The last column in Table I shows that inclusion of the third SVD decomposed signal channel decreases the reconstruction differences to insignificant levels. For the ST analysis in exercise testing, the reconstruction from the two most significant channels appears to be sufficient to acquire the necessary clinical data. In this work, we assessed the effect of residues in other channels, on relevant clinical parameters and fiducial points, like ST levels and J-point. It is shown in Section IV that the reconstruction from the first two decomposed signals provides sufficient accuracy in these clinical parameters.

We also investigated the on-line reconstruction performance of the algorithm, when a channel is lost. Such a case is depicted

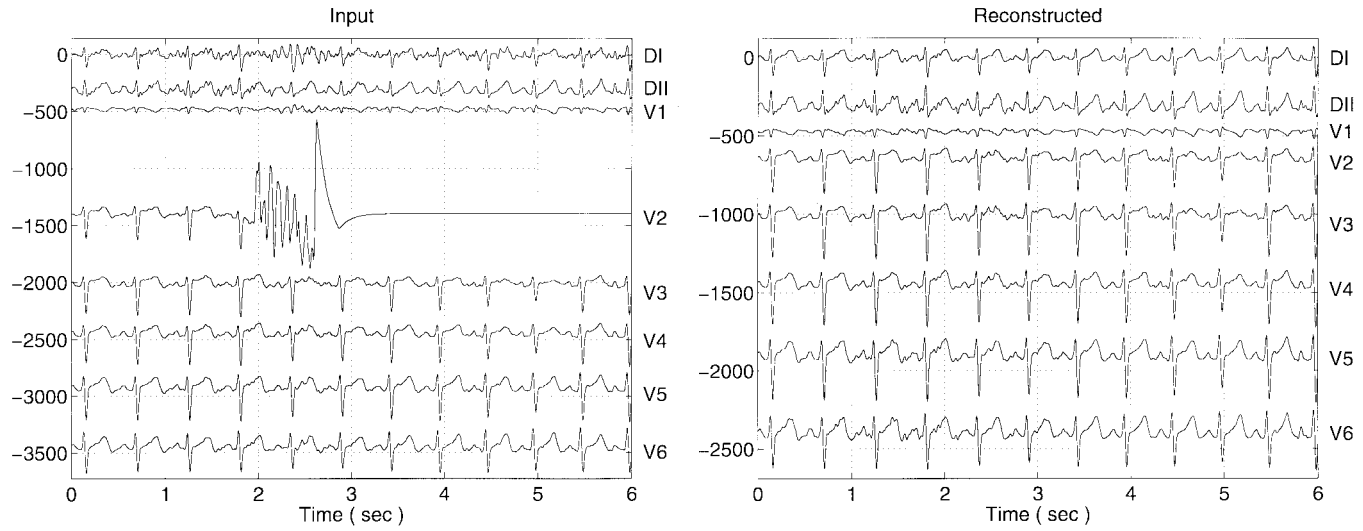

Fig. 7. Complete loss.

TABLE I
PERCENTAGE DIFFERENCES IN RECONSTRUCTION FROM TWO AND THREE SVD-DECOMPOSED CHANNELS

Chn.	*2 Chn. Rec.*	*3 Chn. Rec.*
DI	3.64 %	1.91 %
DII	2.33 %	0.63 %
V1	0.76 %	0.59 %
V2	0.19 %	0.18 %
V3	0.14 %	0.08 %
V4	0.32 %	0.11 %
V5	1.02 %	0.41 %
V6	1.72 %	1.60 %

in Fig. 7 where V2 is lost. When the ECG information in a particular channel is completely lost, the dimension of the algorithm is reduced by one and this channel is excluded from the input. The ECG information unique to that channel cannot be available anymore, obviously. As a consequence, an error in reconstructing the lost channel occurs, which will be equal to the amount of information uniquely contained in that channel. This is observed as a decrease in the singular values of the signal space.

IV. RESULTS AND OBSERVATIONS

Processing is performed by a software that automatically implements recursive SVD and all of the methods and precautions explained in Section III.

The forgetting factor, α, determines how far the algorithm remembers past data. The values of α that can be used for ECG data must be less than but close to unity. If it is too close to one, the algorithm loses its adaptability. If it is too low, the algorithm becomes highly unstable and cannot preserve the ECG signal morphology. In such cases, even the regular QRS complexes can cause high rotations of $\mathbf{u}$ vectors, as if they are uncorrelated with the past data. Different values of α are tested on the data set. It has been observed that the decomposed waveforms are quite insensitive to the values of α between $1-2^{-10}$ and $1-2^{-16}$. A good compromise is obtained with $\alpha = 1-2^{-13}$.

The algorithm is sensitive to DC or very low-frequency components as mentioned previously. Care must be taken to remove all of the low-frequency components, frequency of which is less than the filtering effect of the forgetting factor α.

The performance of the method is tested from two different points of view, the ST-segments' information content and the preservation of the J-point.

Assessment of the results of the proposed method can only be done by testing the method on real data. Hence the following testing methodology for the reliability of ST-segment and J-point measurements is adopted.

1) Standard ECG derivations are reconstructed from only the two most significant decomposed signal channels.
2) ST-segment level and J-point measurements are made on these reconstructed signals.
3) These measurements are compared to the measurements made on the original data by standard methods.

The ST measurements were done on average beats calculated from every six-second interval, on both of the original and the reconstructed signal records. Our software detects every QRS complex and aligns these for maximum cross-correlation. Beats with low correlation are not taken into averages. Reconstruction is made from the two most significant SVD decomposed signal channels. Although ST measurements for each beat could have been made in the reconstructed channel, this was not possible for the original channel. Interference in the original signal prohibits direct calculation of ST levels. When complexes are chosen for averaging in any six-second interval on the original data, a correlation-based acceptance and alignment criteria is used (which is quite common in many commercial stress test systems). Hence only those complexes with reasonably low interference, in the original data, are included in the average complexes. The comparison was based on the measurements made on average complexes.

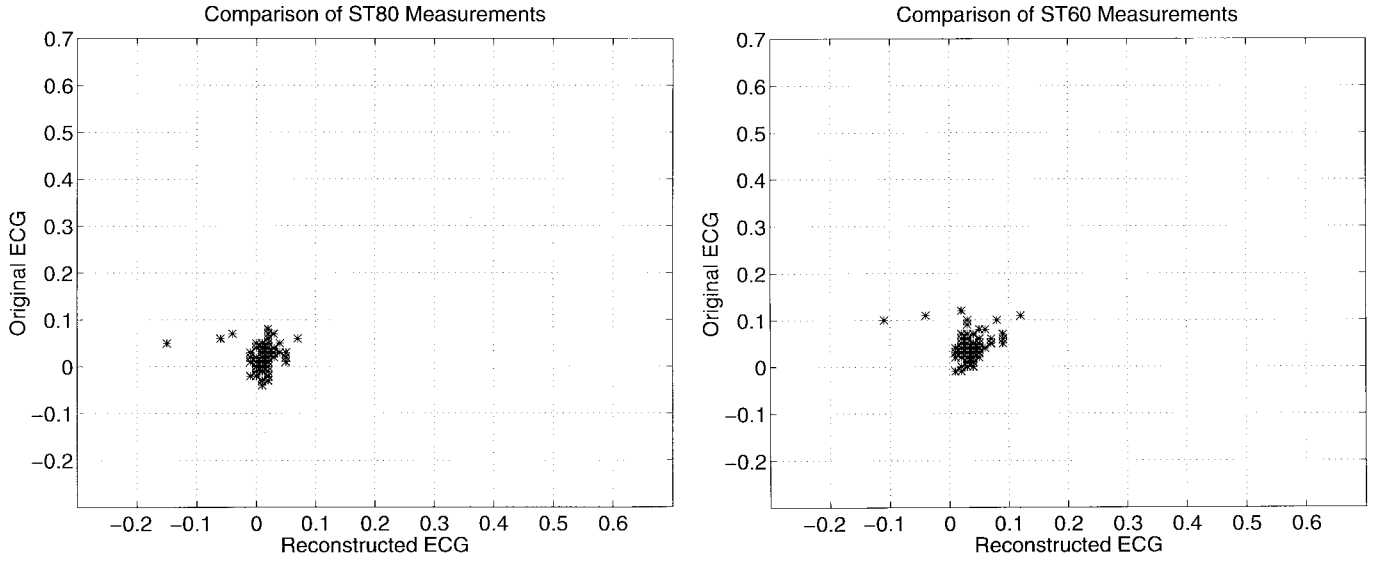

Fig. 8. ST measurements from normal ECG (both axes are in mV).

Two ST measurements were taken from each average beat, 60 and 80 ms after the J-point. They are named ST60 and ST80, respectively. These measurements are compared using linear regression analysis. The model used is $y_i = a \times x_i + b$, where y_i's and x_i's are the ST measurements from the original and the reconstructed data, respectively. The locations of the J-points in each average beat were also recorded.

A normal ECG does not exhibit any ST-level shift. Hence the corresponding ST measurements have very low variance. Fig. 8 shows the comparison of ST80 and ST60 measurements for a typical patient with no ST-level shift. There are 106 data points in these figures. The small variance in both of the data sets shows that the ST-segments are preserved quite well. The results are similar in all channels and for all normal ECG records. The improvement in the data quality can also be observed by comparing the number of accepted QRS complexes in the reconstructed and the original signals. On the average, there is 8.5% increase in the number of accepted QRS complexes in the reconstructed signals.

The abnormal ECG exhibits ST-level elevation or depression. The important information in ST analysis is the trend of the ST level. The linear regression analysis (LRA) between the measurements from the original and the reconstructed data gives a good measure of how well the trend is preserved. The closeness of the slope of the regression line to one shows how well the ST measurements fit to each other. The discontinuities in the ST measurements on the original data caused by the presence of high levels of unwanted signal components are also removed in the reconstructed data. Fig. 9 shows a comparison of the ST80 in all of the eight derivations of a patient's data when there is ST-level shift. There is significant ST-segment variation in the derivations DII and V2–V6 whereas in DI and V1 there is no ST-segment variation. In the data set of 23 patients, 10 contained ST-segment variation in some of their derivations. Whenever there is a significant ST-segment variation, regression slope resulted very close to 1.00. For the above patient, slope is 0.84 for DI, 0.86 for DII, 0.93 for V1, 0.96 for V2, 0.98 for V3, 0.99 for V4, 1.00 for V5 and 0.90 for V6. When there is no ST-segment variation, like in channels DI and V1 in Fig. 9, slope may deviate from 1.00. The data points are confined in a small region in such cases, indicating a good fit. Linear regression is not an appropriate measure for such data.

We evaluated the average distance between the regression line, $y = a \times x + b$, and the data points (x_i, y_i) for every channel and for every patient. This measure shows the deviation of the data pairs, original and reconstructed, from the regression line. The individual distance between (x_i, y_i) and the regression line for a derivation of a patient record is

$$d_i = \sqrt{(x_i - x_n)^2 + (y_i - y_n)^2}. \tag{22}$$

Here, (x_n, y_n) is the point on $(y = a \times x + b)$ where the normal from (x_i, y_i) intersects this line. Average distance is then calculated as

$$\overline{d} = \frac{1}{K} \sum_{k=1}^{K} \left(\frac{1}{8} \sum_{j=1}^{8} \left(\frac{1}{N} \sum_{i=1}^{N} (d_{ijk}) \right) \right) \tag{23}$$

where i indicates the ST-level measurements, j indicates the derivation, and k indicates the patient. The average distance calculated is 30.0 μV over the population of 22 patients. One record has particularly high-amplitude unwanted signal components and for this record the average distance is 125.3 μV, over all derivations.

The J-points are important in ST analysis. Any error in locating the J-point causes wrong ST measurements. We determined the location of the J-point in each average beat. A comparison of the locations of the J-points showed that our method does not introduce any bias on the J-points and, thus, does not degrade the performance of the ST analysis. Table II shows the average difference in locations, in milliseconds, between the original and the reconstructed data. The relatively higher differences correspond to data with high unwanted signal interference in the original signal.

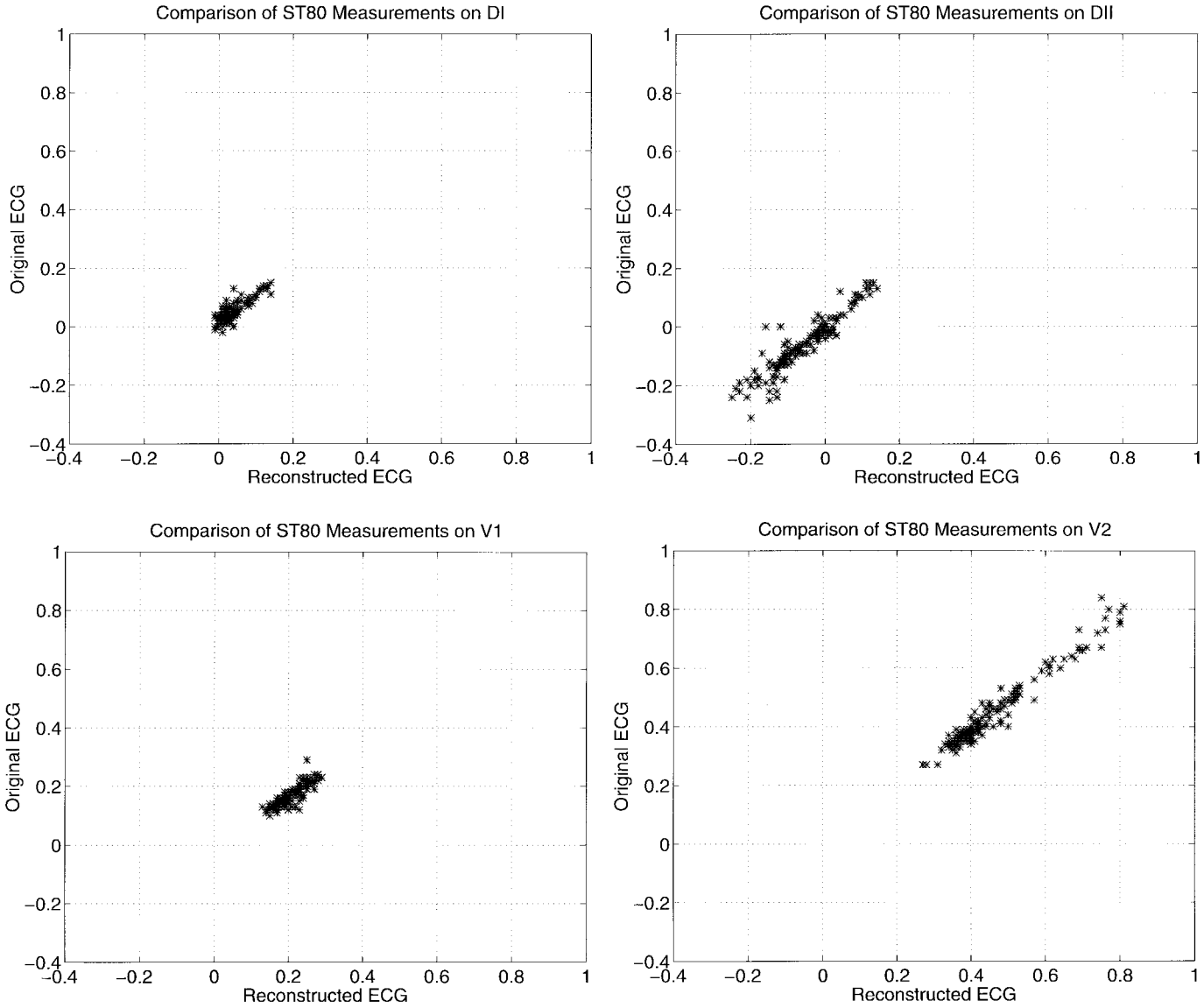

Fig. 9. ST measurements from abnormal ECG (both axes are in mV).

TABLE II
DIFFERENCE IN J-POINT LOCATIONS (IN MS)

Patient	Difference	Patient	Difference	Patient	Difference
1	4.2	2	0.5	3	2.0
4	5.8	5	0.6	6	1.4
7	3.1	8	2.6	9	1.8
10	2.2	11	10.0	12	0.8
13	0.9	14	0.7	15	1.0
16	0.9	17	0.9	18	4.0
19	0.6	20	1.0	21	0.5
22	0.7	23	1.6		

We also compared the J-point amplitude measurements done on the resting phase of each patient data. The average mean square errors of the J-point amplitudes measured over the entire data set are as follows: DI: 3.93%, DII: 8.08%, V1: 1.33%, V2: 1.45%, V3: 0.98%, V4: 4.38%, V5: 1.54%, V6: 2.40%.

V. CONCLUSION

In this paper we presented a method for processing the exercise ECG records in real-time, on Pentium microprocessor-based computers. This method employs SVD in an algorithm, which automatically separates ECG data from time-orthogonal interfering signals. Also it reconstructs the lost input channels from the information contained in other channels in standard 12-lead ECG.

The method makes use of the redundancy in the recorded data in order to secure the extraction of maximum clinical information. It is observed that most of the ECG signal energy is contained in the first two decomposed channels. The reconstruction of the ST-segment only from these channels yields very accurate measurements. It is also observed that

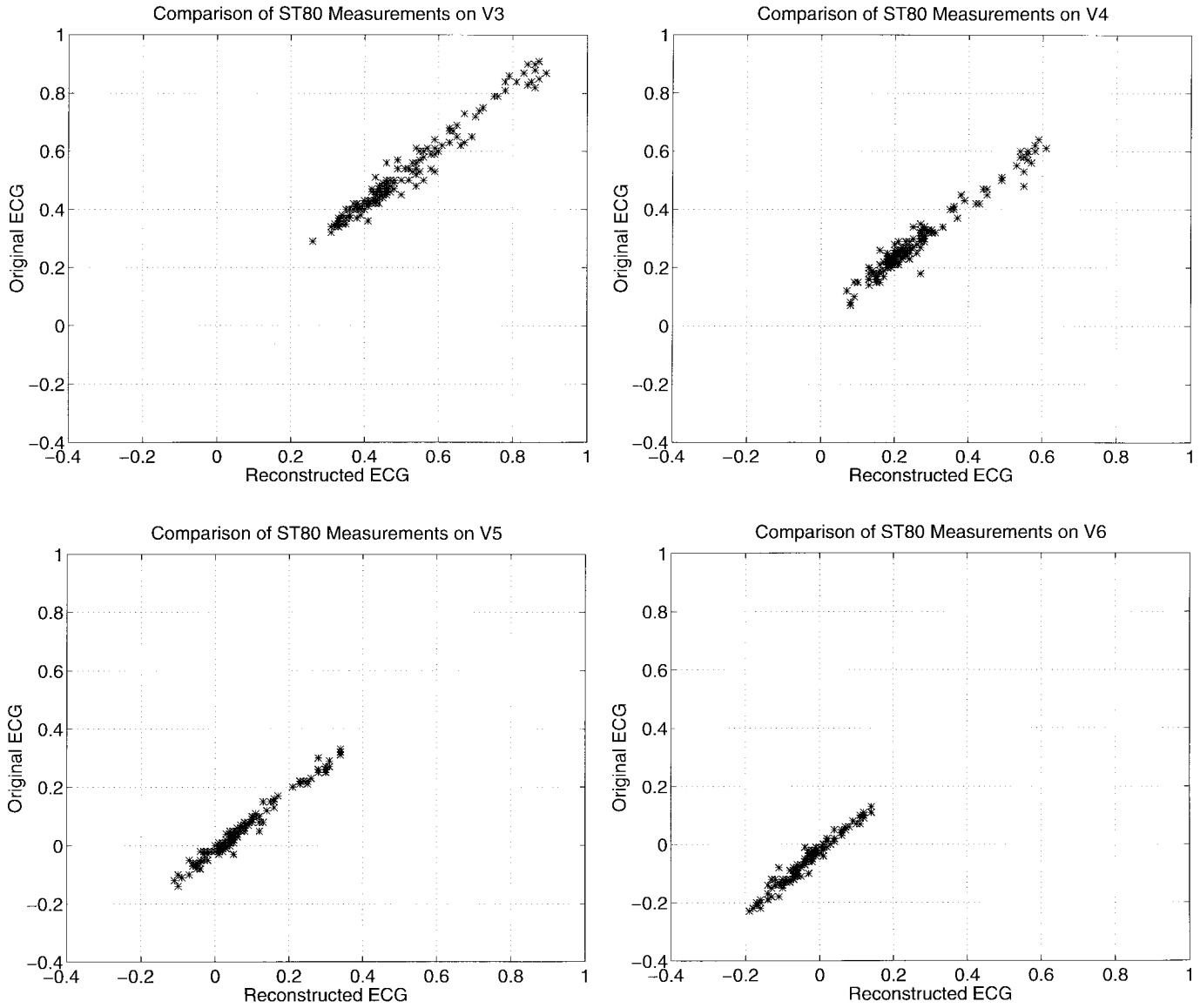

Fig. 9. (*Continued*.) ST measurements from abnormal ECG (both axes are in mV).

the dimension of signal space does not exceed three. It is shown in this paper that ST-segment level variation can be accurately measured by using reconstructed derivations from only the most significant two time-orthogonal signals. These two signals are shown to be quite immune to interference from BW and EMG and, hence, the ST levels, thus, obtained are very reliable.

The SVD decomposed signal channels preserve all the clinically significant data. It is shown in this paper that loss of any one of the channels can be recovered from other channels. The accuracy is determined by the amount of redundancy in the signal set.

Exercise ECG signals contain many unwanted signal components and artifacts. Besides, the morphology of ECG data of a patient changes significantly during the course of the test. Our method employs this redundancy to separate unwanted signal components from the clinically useful data.

A completely automatic algorithm is presented. The performance and the limitations of this method are discussed. The method and the various limits and the thresholds used are tested on 23 patient records. The method needs further testing on a larger exercise data set. This is necessary to improve the criteria for precision and for robustness. The performance of the method must also be assessed for the value and the position of all fiducial points on ECG. In this work, this assessment is limited to the J-point and the ST-segment.

A statistical assessment of errors committed in reconstructing a completely lost channel must also be made on a larger data set.

As far as the decomposed signal set is concerned, a unique dependence on DII is observed. This is the only channel that records ECG along the vertical axis of the heart, and it is less correlated to other channels. A larger part of the information contained in this channel cannot be recovered from other

channels. Any unwanted signal component that contaminates DII affects the signal space components of the decomposed signal set significantly. An extra redundancy is necessary, in order to improve the performance of the method against such contamination in DII. This can be maintained by recording DIII independently.

REFERENCES

[1] V. X. Afonso, W. J. Tompkins, T. Q. Nguyen, K. Michler, and S. Luo, "Comparing stress ECG enhancement algorithms," *IEEE Eng. Med. Biol.y Mag.*, vol. 15, pp. 37–44, May/June 1996.

[2] P. P. Kanjilal, S. Palit, and G. Saha, "Fetal ECG extraction from single-channel maternal ECG using singular value decomposition," *IIEEE Trans. Biomed. Eng.*, vol. 44, pp. 51–59, Jan. 1997.

[3] A. Van Oosterom, "Spatial filtering of the fetal electrocardiogram," *J. Perinatal Med.*, vol. 14, pp. 411–419, 1986.

[4] J. H. Van Bemmel, "Detection of weak electrocardiograms by autocorrelation and cross correlation envelopes," *IIEEE Trans. Biomed. Eng.*, vol. BME-15, pp. 17–23, 1968.

[5] R. L. Longini, T. A. Reichert, J. M. Yu, and J. S. Crowley, "Near-orthogonal basis functions: A real-time fetal ECG technique," *IEEE Trans. Biomed. Eng.*, vol. BME-24, pp. 39–43, 1977.

[6] C. Li, C. Zheng, and C. Tai, "Detection of ECG characteristic points using wavelet transform," *IEEE Trans. Biomed. Eng.*, vol. 42, pp. 21–28, Jan. 1995.

[7] D. A. Coast, R. M. Stern, G. G. Cano, and S. A. Briller, "An approach to cardiac arrhythmia analysis using hidden Markov model," *IEEE Trans. Biomed. Eng.*, vol. 37, pp. 826–836, 1990.

[8] J. Pan and W. J. Tompkins, "A real-time QRS detection algorithm," *IEEE Trans. Biomed. Eng.*, vol. BME-32, pp. 230–236, Mar. 1985.

[9] N. Ahmed, P. J. Milne, and S. G. Harris, "Electrocardiographic data compression via orthogonal transforms," *IEEE Trans. Biomed. Eng.*, vol. BME-23, pp. 484–487, 1975.

[10] D. Callaerts, B. De Moor, J. Vandewalle, W. Sansen, G. Vantrappen, and J. Janssens, "Comparison of SVD methods to extract the fetal electrocardiogram from cutaneous electrode signals," *Med. Biol. Eng.. Comput.*, vol. 28, pp. 217–224, 1990.

[11] I. S. N. Murthy and G. S. S. Durga Prasad, "Analysis of ECG from pole-zero models," *IEEE Trans. Biomed. Eng.*, vol. BME-39, pp. 741–751, 1992.

[12] J. Mertens and D. Mortara, "A new algorithm for QRS averaging," in *Proc. Comput. Cardiol.*, 1984, pp. 367–369.

[13] V. Pinto, "Filters for the reduction of baseline wander and muscle artifact in the ECG," *J. Electrocardiol.*, vol. 25, pp. 40–48, 1992.

[14] L. Sornmo, "Time-varying filtering for removal of baseline wander in exercise ECG's," in *Proc. Comput. Cardiol.*, 1991, pp. 145–148.

[15] D. W. Mortara, "Source consistency filtering—A new tool for ECG noise reduction," in *Proc Comput. Cardiol. Proceedings*, 1991, pp. 125–128.

[16] R. Jane, P. Laguna, N. V. Thakor, and P. Caminal, "Adaptive baseline wander removal in the ECG: Comparative analysis with cubic spline technique," in *Proc. Comput. Cardiol.*, 1992, pp. 143–146.

[17] C. R. Meyer and H. N. Keiser, "Electrocardiogram baseline noise estimation and removal using cubic splines and state computation techniques," *Comput. Biomed. Res.*, vol. 10, pp. 459–470, 1977.

[18] V. X. Afonso, W. J. Tompkins, T. Q. Nguyen, S. Trautmann, and S. Luo, "Filter bank-based processing of the stress ECG," presented at *Proc. Annu. Int. Conf. IEEE Eng. Med. Biol. Soc.*, Sept. 1995.

[19] R. C. Barr, M. S. Spach, and G. S. Herman-Giddens, "Selection of the number and positions of measuring locations for electrocardiography," *IEEE Trans. Biomed. Eng.*, vol. BME-18, pp. 125–138, 1971.

[20] R. L. Lux, A. K. Evans, M. J. Burgess, R. F. Wyatt, and J. A. Abildskov, "Redundancy reduction for improved display and analysis of body surface potential maps—I: Spatial compression," *Circ. Res.*, vol. 49, no. 1, pp. 186–196, 1981.

[21] A. K. Evans, R. L. Lux, M. J. Burgess, R. F. Wyatt, and J. A. Abildskov, "Redundancy reduction for improved display and analysis of body surface potential maps—II: Temporal compression," *Circ. Res.*, vol. 49, no. 1, pp. 197–203, 1981.

[22] J. Vanderschoot, D. Callaerts, W. Sansen, J. Vandewalle, G. Vantrappen, and J. Janssens, "Two methods for optimal MECG elimination and FECG detection from skin electrode signals," *IEEE Trans. Biomed. Eng.*, vol. BME-34, pp. 233–243, 1987.

[23] G. H. Golub and C. F. Van Loan, *Matrix Computations.* Baltimore, MD: Johns Hopkins Univ. Press, 1989, pp. 70–73.

[24] ———, *Matrix Computations.* Baltimore, MD: Johns Hopkins Univ. Press, 1989, pp. 445–448.

[25] ———, *Matrix Computations.* Baltimore, MD: Johns Hopkins Univ. Press, 1989, pp. 246–248.

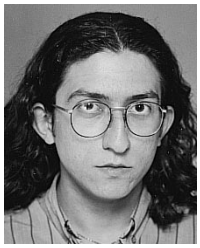

Burak Acar was born in Izmir, Turkey, on October 24, 1972. He received the B.Sc. and M.Sc. degrees from Bilkent University, Ankara, Turkey, both in electrical and electronics engineering. As part of his ongoing Ph.D. degree studies at Bilkent University, he is currently conducting research into ECG analysis at the Cardiological Sciences Department of St. George's Hospital Medical School, London, U.K.

His current research area is personal-computer-based ECG signal acquisition and processing.

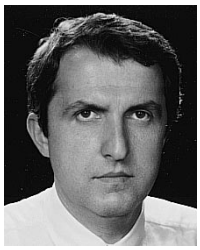

Hayrettin Köymen (S'74–M'87–SM'91) was born in Ankara, Turkey, on June 7, 1952. He received the B.Sc. and M.Sc. degrees from the Middle East Technical University, Ankara, Turkey, in 1973 and 1976, respectively, and the Ph.D. degree from the University of Birmingham, Birmingham, U.K., in 1979, all in electrical engineering.

In 1979, he became a Faculty Member of the Middle East Technical University. Until 1982, his work involved underwater acoustics and oceanographic instrumentation. Since 1982, his work has involved physiological signal acquisition and processing, medical ultrasonics, and ultrasonic nondestructive evaluation. In 1990, he joined the faculty of Bilkent University, Ankara, where he is now a Professor in the Department of Electrical and Electronics Engineering. His current research interests are personal computer-based biomedical signal acquisition and processing, medical imaging, finite amplitude effects in medical ultrasonics, and acoustic microscopy using leaky waves in layered media.